PHYSICAL REVIEW E **75**, 040701(R) (2007)

Dynamic electric polarization of nematic liquid crystals subjected to a shear flow

Stefan Grandner,[1] Sebastian Heidenreich,[1,*] Patrick Ilg,[1,2] Sabine H. L. Klapp,[1,3] and Siegfried Hess[1]
[1]*Institute for Theoretical Physics, Technische Universität Berlin, Hardenbergstrasse 36, D-10623 Berlin, Germany*
[2]*Institute for Polymers, ETH Zuerich, Wolfgang-Pauli-Str. 10, 8093 Zuerich*
[3]*Stranski-Laboratorium for Physical and Theoretical Chemistry, Technische Universität Berlin, Strasse des 17. Juni 115, D-10623 Berlin, Germany*

(Received 11 September 2006; published 6 April 2007)

The effect of coupling between the dipole moment and the orientation is explored based on a relaxation equation for the second rank alignment tensor characterizing the molecular order in liquid crystals and a corresponding equation for the electric polarization. The orientational dynamics leads to a time dependence of the electric polarization. We propose a possibility to measure these effects via the resulting magnetic fields of the magnitude $|\mathbf{B}| \approx 10^{-9}$ T. Furthermore, the presence of the electric polarization modifies the orientational dynamics as demonstrated in solution phase diagrams.

DOI: 10.1103/PhysRevE.75.040701 PACS number(s): 61.30.Gd, 47.57.Lj, 61.30.Cz, 95.10.Fh

I. INTRODUCTION

Many liquid crystalline substances are composed of molecules with a permanent electric dipole moment. Yet due to directional averaging, there is no electric polarization in a spatially homogeneous nematic state in equilibrium. In the presence of a shear flow the alignment tensor characterizing the orientation of the back bone (figure axis) performs damped and undamped oscillations, as in tumbling nematics [1–3]. Even chaotic behavior is possible [4–8]. The dynamics of the alignment leads to a dynamic behavior of the electric polarization which is proportional to the average electric dipole moment. In this Rapid Communication, the theory of the coupled dynamics of the electric polarization vector and of the second rank alignment tensor of tumbling nematic liquid crystals [5,6] is treated. To rationalize the underlying static coupling we use density-functional arguments [9–12]. The basic equations are formulated and numerical results are presented for selected values of the relevant model parameters where the orientational behavior is distinctively different from the previously studied systems without dipole moment [4–8]. Dielectric polarization has been measured in the nematic liquid crystal 6*CB* in [13]. The shear flow-induced polarization in ferroelectric smetic-*C* liquid crystals [14] is associated with physical properties which are absent in *a*-chiral nematics. The influence of an external magnetic field on the orientational dynamics was recently studied in [15].

II. MODEL EQUATIONS

The macroscopic variables describing the orientation of the (back bone of the) molecule and of the electric dipole moment are the second rank alignment tensor $\mathbf{a}$ and the dipole vector $\mathbf{d}$. They are defined by $\mathbf{a}=\sqrt{\frac{15}{2}}\langle\overline{\mathbf{uu}}\rangle$ and $\mathbf{d}=\langle\mathbf{e}\rangle$. Here $\mathbf{u}$ is the unit vector parallel to the figure axis of the molecule. The symbol $\bar{\mathbf{x}}$ indicates the symmetric traceless part of a tensor $\mathbf{x}$. The molecular dipole moment $\mathbf{p}$ is written as $\mathbf{p}=p^{el}\mathbf{e}$ with the magnitude p^{el} and its direction is determined by the unit vector $\mathbf{e}$. The averages $\langle\cdots\rangle$ are evaluated with an orientational distribution function which need not be specified here. Notice that the molecule is a biaxial object unless $\mathbf{e}$ is parallel to $\mathbf{u}$.

The symmetric traceless part $\bar{\boldsymbol{\epsilon}}$ of the dielectric tensor $\boldsymbol{\epsilon}$ is $\bar{\boldsymbol{\epsilon}}=\varepsilon_a\mathbf{a}$, with the coefficient ε_a specifying the optical anisotropy of the molecule. The shear flow-induced modifications of the alignment can be detected optically [16]. The electric polarization $\mathbf{P}$ is related to the dipole vector by $\mathbf{P}=\rho\langle\mathbf{p}\rangle=\rho p^{el}\mathbf{d}$, where ρ is the number density. The direct measurement of $\mathbf{P}$ is, in principle, possible as we later show. In the original theoretical approach a nonlinear relaxation equation for the alignment tensor $\mathbf{a}$, coupled to the velocity gradient field, was derived [17]. In this Rapid Communication we consider the obvious extension to a coupling with a dipolar vector for a spatially homogeneous situation. The modeling is akin to the two-alignment-tensor theory used for polymeric side chain liquid crystals [18].

The equations involve characteristic phenomenological coefficients; these are the relaxation time coefficients $\tau_a>0$ and $\tau_d>0$, as well as τ_{ap} which determines the strength of the coupling between the alignment and the pressure tensor or the velocity gradient, and the dimensionless coefficients κ and κ_d. Furthermore, derivatives of a generalized Landau–de Gennes (LG) potential $\Phi=\Phi(\mathbf{a},\mathbf{d})$ with respect to $\mathbf{a}$ and $\mathbf{d}$ occur in these equations. Here we write the (dimensionless) potential function as $\Phi=\Phi^a(\mathbf{a})+\Phi^d(\mathbf{d})+\frac{1}{2}c_0\mathbf{d}\cdot\mathbf{a}\cdot\mathbf{d}$, with the coefficient c_0 characterizing the strength of the simplest type of coupling between the vector $\mathbf{d}$ and the second rank tensor $\mathbf{a}$. The flexoelectric coupling which is linear in $\mathbf{d}$ requires a spatially inhomogeneous situation which is not considered here. For the function Φ^a the standard expression [17] $\Phi^a=(1/2)A(T)\mathbf{a}:\mathbf{a}-(1/3)\sqrt{6}B(\mathbf{a}\cdot\mathbf{a}):\mathbf{a}+(1/4)C(\mathbf{a}:\mathbf{a})^2$ is used with $A(T)=A_0(1-T^*/T)$. The pseudocritical temperature T^*, the nematic-isotropic transition temperature T_K with $T_K>T^*$, and the positive coefficients A_0, B, C [with $C<2B^2/(9A_0)$] are model parameters. The value of A_0 depends, in principle, on the proportionality coefficient chosen between $\mathbf{a}$ and $\langle\overline{\mathbf{uu}}\rangle$. The choice made above implies $A_0=1$,

*Corresponding author. Electronic address: sebastian@itp.physik.tu-berlin.de

cf. [17]. We note that all these coefficients are linked to measurable quantities and can also be related to molecular quantities within the framework of a mesoscopic theory [19–21]. An amended expression for the LG potential has been introduced and analyzed in [22]. For the plane Couette flow to be studied here the observable differences are not crucial, thus we use the simpler expression here. The potential function associated with the dipolar vector, however, is chosen such that the magnitude of $\mathbf{d}$ is bounded, specifically: $\Phi^d = \frac{1}{2}A_d \mathbf{d}\cdot\mathbf{d} - \frac{1}{4}E\ln[1-(\mathbf{d}\cdot\mathbf{d})^2]$, with positive and temperature-independent coefficients A_d and E. The condition $A_d > 0$ implies that there is no spontaneous polarization. Computation of the dipolar vector in the presence of an orienting electric field with the potential used here and comparison with the corresponding expression given by the Langevin function yields $A_d = 3$ and, to a good approximation, $E \approx 3$, for uncorrelated particles.

The equation resulting for the change of the alignment tensor $\mathbf{a}$ in the presence of a flow field $\mathbf{v}$ reads [17,23]

$$\frac{\partial \mathbf{a}}{\partial t} - 2\overline{\boldsymbol{\Omega}\times\mathbf{a}} - 2\kappa\overline{\boldsymbol{\Gamma}\cdot\mathbf{a}} + \tau_a^{-1}\boldsymbol{\Phi}^a(\mathbf{a},\mathbf{d}) = -\sqrt{2}\frac{\tau_{ap}}{\tau_a}\boldsymbol{\Gamma}. \quad (1)$$

The analogous equation for the vector $\mathbf{d}$ is given as

$$\frac{\partial \mathbf{d}}{\partial t} - \boldsymbol{\Omega}\times\mathbf{d} - \kappa_d\boldsymbol{\Gamma}\cdot\mathbf{d} + \tau_d^{-1}\boldsymbol{\Phi}^d(\mathbf{a},\mathbf{d}) = 0. \quad (2)$$

Here, the derivatives of the LG potential are given as $\boldsymbol{\Phi}^a(\mathbf{a}) \equiv \partial\Phi/\partial\mathbf{a} = A\mathbf{a} - \sqrt{6}B\overline{\mathbf{a}\cdot\mathbf{a}} + C\mathbf{a}\mathbf{a}:\mathbf{a} + \frac{1}{2}c_0\overline{\mathbf{d}\mathbf{d}}$, $\boldsymbol{\Phi}^d(\mathbf{a},\mathbf{d}) \equiv \partial\Phi/\partial\mathbf{d} = A_d\mathbf{d} + E\mathbf{d}(\mathbf{d}\cdot\mathbf{d})/[1-(\mathbf{d}\cdot\mathbf{d})^2] + c_0\mathbf{a}\cdot\mathbf{d}$. The symbols $\boldsymbol{\Gamma}$ and $\boldsymbol{\Omega}$ denote the symmetric traceless part of the velocity gradient tensor (strain rate tensor) $\boldsymbol{\Gamma} \equiv \overline{\nabla\mathbf{v}}$, and the vorticity $\boldsymbol{\Omega} \equiv (\nabla\times\mathbf{v})/2$, respectively. In the following analysis we specialize on a simple shear flow. In the case of a plane Couette flow, nonzero values of the parameter κ induce quantitative but practically no qualitative changes in the dynamics of the alignment (as compared to $\kappa = 0$) [5,6]. Therefore we set $\kappa = \kappa_d = 0$ in the following.

The entropic part of the free energy F^{or}, involving the one-particle orientational distribution function, leads to the value $c_0 = -3(6/5)^{1/2}P_2(\mathbf{e}\cdot\mathbf{u})$ for the coupling coefficient. The above result, especially the coupling term, follows from a Taylor expansion of F^{or} around the isotropic case [9–12]. Additional contributions to the coupling coefficient may arise from molecular correlations which, in principle, could be handled within a density functional ansatz [9–12]. The electric polarization is preferentially parallel and perpendicular to the nematic director for $c_0 < 0$ and $c_0 > 0$, respectively.

Equations (1) and (2) can be rewritten in scaled variables [17,23–25]. The alignment tensor and the dipolar vector are expressed in units of the value of the order parameter at the isotropic-nematic transition, $a_K = (2/3)B/C$. This implies $d^* = d/a_K$ and $a^* = a/a_K$. The scaled temperature is $\vartheta = (1-T^*/T)(1-T^*/T_K)^{-1} = a_K A\Phi_{ref}^{-1}$, where ϕ_{ref} is defined as $\phi_{ref} = (2/9)a_K B^2/C$. In analogy to the reduced temperature ϑ the parameter ϑ_d is given by $a_K A_d \Phi_{ref}^{-1}$, furthermore $E^* = a_K^3 E\phi_{ref}^{-1}$. The relaxation time of the alignment in the isotropic phase $\tau_{ref} = \tau_a A_0^{-1}(1-T^*/T_K)^{-1}$ at the coexistence temperature is chosen here as reference time, the shear rate is given by $\dot{\gamma}^* = \dot{\gamma}\tau_{ref}$. Furthermore, the coupling coefficient is related to c_0 by $a_K^2 c_0 = \phi_{ref} c$. Instead of the ratio τ_{ap}/τ_a the parameter $\lambda_K = -2/3\sqrt{3}\tau_{ap}/\tau_a a_K^{-1}$ is used, as in [5,6,8].

The derivatives $\boldsymbol{\Phi}^a$ and $\boldsymbol{\Phi}^d$ of the potential function in Eq. (1) can be written as

$$\boldsymbol{\Phi}^{a*}(\mathbf{a}^*,\mathbf{d}^*) = \vartheta\mathbf{a}^* - 3\sqrt{6}\,\overline{\mathbf{a}^*\cdot\mathbf{a}^*} + 2\mathbf{a}^*\mathbf{a}^*:\mathbf{a}^* + \tfrac{1}{2}c\overline{\mathbf{d}^*\cdot\mathbf{d}^*},$$

$$\boldsymbol{\Phi}^{d*}(\mathbf{a}^*,\mathbf{d}^*) = \vartheta_d\mathbf{d}^* + E^*\mathbf{d}^*(\mathbf{d}^*\cdot\mathbf{d}^*)/[1-(\mathbf{d}^*\cdot\mathbf{d}^*)^2/(d_{max}^*)^4] + c\mathbf{a}^*\cdot\mathbf{d}^*.$$

The maximum magnitude of the scaled dipole vector is d_{max}^*. Now quantities in reduced units are denoted by the same symbols as the original ones. The symmetric traceless alignment tensor has five independent components $a_0 \cdots a_4$ [5,6,8]. The components of the dipolar vector are denoted by d_1, d_2, d_3.

The relaxation time τ_a as well as τ_d can be related to the rotational diffusion coefficient by a generalized Fokker-Planck equation (in the spirit of [19]). In that approach the ratio of τ_a/τ_d is fixed by the value 3. Depending on the relevant model parameters $\dot{\gamma}$, λ_K, ϑ, ϑ_d, as well as on the coupling coefficient c the solutions either approach a steady state or are time dependent. Furthermore, solutions which, for long times, maintain the symmetry of the plane Couette type velocity gradient and where the tensor components a_3 and a_4 vanish (in plane) have to be distinguished from symmetry breaking solutions where these components are nonzero (out of plane). In the following we use $E^* = 0.04$; the results are not very sensitive to the value of E^*.

Within the alignment-tensor theory for pure liquid crystals without dipole vectors ($c = 0$), various types of orbits have been found [5]. These are, on one hand, *symmetry-adapted states* referred to as aligning (A), tumbling (T), wagging (W), and log rolling (LR). On the other hand, there are *symmetry breaking states* classified as kayaking-tumbling (KT), kayaking-wagging (KW), and complex (C). The C type includes periodic orbits composed of sequences of KT and KW motion with multiple periodicity as well as aperiodic, erratic orbits. The largest Lyapunov exponent for the latter orbits is positive, i.e., these orbits are *chaotic*.

III. REPRESENTATIVE RESULTS FOR THE DYNAMICS IN THE TUMBLING REGIME

The model equations are solved numerically by a Runge-Kutta-Fehlberg algorithm, with small random initial values of magnitude about 0.1 for the components of $\mathbf{a}$ and $\mathbf{d}$. For $c = 0$ the algorithm was tested in a comparison of the solution phase diagram given in [5]. In the following we focus on dynamics of dipole moments perpendicular ($c > 0$) and parallel ($c < 0$) to the figure axis.

First we consider a KT solution without dipole moment. In this case the eigenvector associated to the main eigenvalue rotates out of the shear plane such that the projection on the shear plane is drawing an ellipse. For liquid crystals with a dipole moment perpendicular to the nematic director

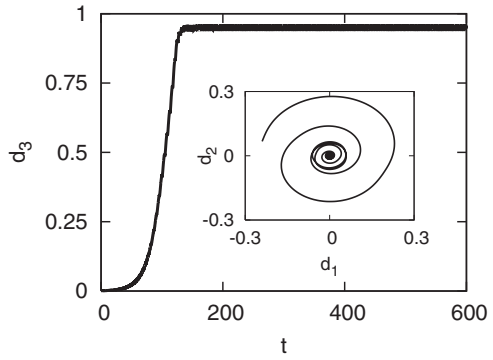

FIG. 1. Phase plots of the dipole vector components d_1 vs d_2 and the time evolution of d_3. The temperature is $\vartheta=0$; the other model parameter are $\lambda_k=1.0$, $\dot{\gamma}=1.9$, $\kappa_d=\kappa=0$, $\vartheta_d=0.1$, $E^*=0.04$, and $c=0.5$.

$(c>0)$, however, the solution becomes unstable in some parameter regions of λ_k, γ_0, and a *KT* to *T* transition can be observed. After some time the values of a_3, a_4 leave the ellipse and go to zero which is characteristic for in-plane solutions (here the *T* solution). A similar behavior is observed for the components of the dipolar vector. In Fig. 1 the dynamics of the dipole vector is illustrated. Whereas the third component reached a stationary value after some time, the components d_1, d_2 go to zero, i.e., the polarization is in the z direction.

In the case where the dipole moment is perpendicular to the figure axis $(c>0)$ the *T* solution is preferred over the *KT* solution. For different initial conditions, especially for very small values for d, we obtained the *KT* instead of the *T* solution. On the other hand for dipole moments parallel to the figure axis $(c<0)$ the *KT* state is favored. As shown in Fig. 2 the tensor components a_3, a_4 grow up to a limit cycle which is characteristic for out-of-plane solutions (in this case *KT*). Here we have a symmetry-breaking effect caused by the dipole moment. This behavior can also be seen from the dynamics of the dipole vector **d**, cf. Fig. 3. At short times the dynamics follows the solution of the uncoupled system $(c=0)$, but after about 1000 time units the component d_3 of the dipole vector approaches a saddle point. Simultaneously, the components d_2 and d_1 leave their limit cycle to reach a smaller stable limit cycle: we observe a transition from *T* to *KT* motion. The remarkable finding is the time dependence of the electric polarization.

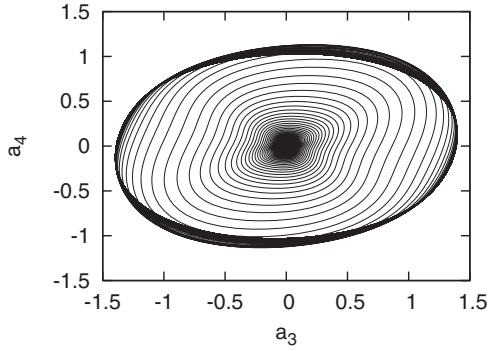

FIG. 2. Phase plots of a_3 vs a_4 at $\vartheta=0$, $\lambda_k=1.0$, $\dot{\gamma}=3.3$, $\kappa_d=\kappa=0$, $\vartheta_d=0.1$, $E^*=0.04$, and $c=-1.0$.

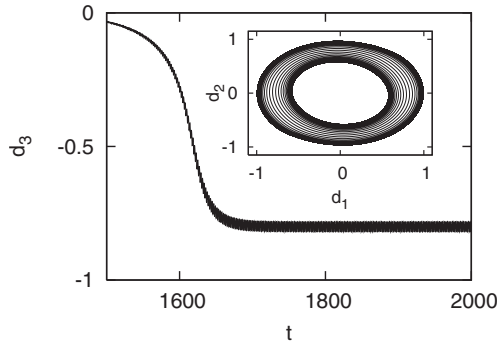

FIG. 3. Phase plots of the dipole vector components d_2 vs d_1 and the time evolution of d_3, parameters as in Fig. 2.

For stronger shear rates, a transition from *A* to *W* solutions are seen. For dipole moments parallel to the figure axis and parameters which are characteristic for flow alignment (*A*) in the case of the uncoupled system the molecules start a *W* motion.

The solution phase diagrams displayed in Fig. 4 show the dependence on the model parameters λ_k and $\dot{\gamma}$ for $\vartheta=0$ and for the dipole coupling coefficients $c=0.5$ (upper diagram) and $c=-0.5$ (lower diagram). Compared with the corresponding diagram without a dipolar coupling [5], for $c<0$ the *KT* solution has shrunken in favor of the *T* solution. On the other hand the change of the *W*, *A*, and *C* regions are very small. Even chaotic solutions could be observed. In the

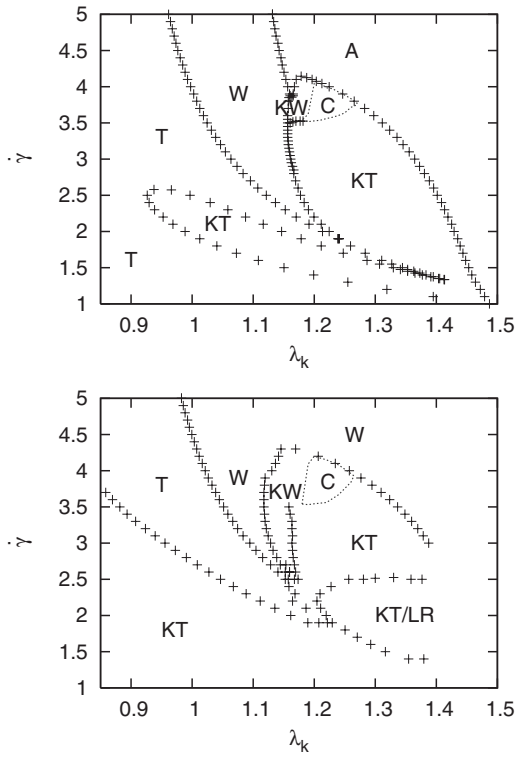

FIG. 4. The solution phase diagram at temperature $\vartheta=0$ for the model parameters $\kappa_d=\kappa=0$, $\vartheta_d=0.1$, and $c=0.5$ for the upper plot and $c=-0.5$ for the lower. The letters are abbreviations for tumbling (*T*), wagging (*W*), kayaking-tumbling (*KT*), kayaking-wagging (*KW*), aligning (*A*), complex (*C*), and log rolling (*LR*).

other case ($c<0$), the *KT* and the *W* is in favor of the *T* and *A* motion, respectively. The transition line from *KT* to *T* solutions is slightly shifted. This shift becomes stronger with increasing coupling strength c.

IV. CONCLUSION

Tumbling nematics with dipole moment show time-dependent electric polarization. On the other hand, the dipole moments in nematic liquid crystal particles affect the dynamics of the orientational order under shear flow as indicated in solution phase diagrams.

Small magnetic fields generated by the time dependent polarization should be measurable. The magnetic field can be inferred from the solution of the wave equation for the vector potential with the inhomogeneity given by $\mu_0\dot{\mathbf{P}}$. For small frequencies and in the near-field regime, where retardation effects are negligible, the magnetic field can also be calculated from the relevant Maxwell equation in the absence of an electric current, $\nabla\times\mathbf{H}=\dot{\mathbf{D}}=\dot{\mathbf{P}}$. As before, a plane Couette flow is considered between flat plates (parallel to the *xz*-plane) separated by the distance h, which is assumed to be very small compared to the length and breadth of the plates. Integration of the Maxwell equation over appropriately chosen areas and use of the Stokes theorem leads to $B_x=-\mu_0\dot{P}_z h/2$ and $B_z=\mu_0\dot{P}_x h/2$ for the tangential components of the **B** field, immediately above the upper plate. An estimate of the field strength is inferred from $|\dot{\mathbf{P}}|=\omega\rho p^{el}|\mathbf{d}|$, where ω is a frequency characteristic for the dynamics of the electric polarization. For $h=10^{-2}$ m, $\omega=10^3$ s^{-1}, $\rho=10^{27}$ m^{-3}, and $p^{el}|\mathbf{d}|=1.610^{-29}$ cm (corresponding to an elementary charge times 10^{-10} m), the field magnitude $|B|\approx 10^{-7}$ T is found. For $h=10^{-3}$ m, $\omega=10^2$ s^{-1} one has $|B|\approx 10^{-9}$ T. The detection limit of a super conducting quantum interference device magnetometer is about 10^{-14} T. So the measurement of the magnetic field generated by the dynamics of the electric polarization in a flowing tumbling nematic liquid crystal is feasible, and it is desirable.

ACKNOWLEDGMENT

We thank Deutsche Forschungsgemeinschaft (DFG) for financial support via the SFB "Mesoskopisch strukturierte Verbundsysteme."

[1] R. G. Larson, *The Structure and Rheology of Complex Fluids* (Oxford University Press, Oxford, UK, 1999).
[2] R. G. Larson and H. C. Öttinger, Macromolecules **24**, 6270 (1991).
[3] M. Kröger, Phys. Rep. **390**, 453 (2004).
[4] M. Grosso, R. Keunings, S. Crescitelli, and P. L. Maffettone, Phys. Rev. Lett. **86**, 3184 (2001).
[5] G. Rienäcker, M. Kröger, and S. Hess, Phys. Rev. E **66**, 040702(R) (2002); Physica A **315**, 537 (2002).
[6] S. Hess and M. Kröger, J. Phys.: Condens. Matter **16**, 3835 (2004); in *Computer Simulations Bridging Liquid Crystals and Polymers*, edited by P. Pasini, C. Zannoni, and S. Zumer (Kluwer, Dordrecht, 2005).
[7] M. G. Forest, Q. Wang, and R. Zhou, Rheol. Acta **86**, 80 (2004).
[8] B. Chakrabarti, M. Das, C. Dasgupta, S. Ramaswamy, and A. K. Sood, Phys. Rev. Lett. **92**, 055501 (2004).
[9] S. H. L. Klapp, J. Phys.: Condens. Matter **17**, R525 (2005).
[10] G. M. Range and S. H. L. Klapp, Phys. Rev. E **69**, 041201 (2004); **70**, 031201 (2004).
[11] S. H. L. Klapp and F. Forstmann, Europhys. Lett. **38**, 663 (1997).
[12] B. Groh and S. Dietrich, Phys. Rev. Lett. **72**, 2422 (1994); Phys. Rev. E **50**, 3814 (1994).
[13] J. Jadzyn, G. Czechowski, and D. Bauman, Z. Naturforsch., A: Phys. Sci. **55a**, 810 (2000).
[14] P. Pieranski, E. Guyon, and P. Keller, J. Phys. (France) **36**, 67 (1975).
[15] M. G. Forest, S. Sicar, Q. Wang, and R. Zhou, Phys. Fluids **18**, 103102 (2006).
[16] G. G. Fuller, *Optical Rheometry of Complex Fluids* (Oxford University Press, New York, 1995).
[17] S. Hess, Z. Naturforsch. A **30a**, 728 (1975).
[18] S. Hess and P. Ilg, Rheol. Acta **44**, 465 (2005); P. Ilg and S. Hess, J. Non-Newtonian Fluid Mech. **134**, 2 (2006).
[19] S. Hess, Z. Naturforsch. A **31a**, 1034 (1976).
[20] S. Hess, in *Electro-optics and Dielectrics of Macromolecules and Colloids*, edited by B. R. Jennings (Plenum, New York, 1979).
[21] M. Doi, Ferroelectrics **30**, 247 (1980); J. Polym. Sci., Polym. Phys. Ed. **19**, 229 (1981).
[22] S. Heidenreich, P. Ilg, and S. Hess, Phys. Rev. E **73**, 061710 (2006).
[23] C. Pereira Borgmeyer and S. Hess, J. Non-Equilib. Thermodyn. **20**, 359 (1995).
[24] S. Hess and I. Pardowitz, Z. Naturforsch. A **36a**, 554 (1981).
[25] G. Rienäcker and S. Hess, Physica A **267**, 294 (1999).